doi: 10.5028/jatm.v6i1.268

Effect of Varying Design Options on the Transient Behavior of a Hybrid Rocket Motor

Raed Kafafy[1], Muhammad Hanafi Azami[1], Moumen Idres[1]

ABSTRACT: Hybrid rockets provide compelling features for use in atmospheric and space rocket propulsion. One of the prominent applications of hybrid rockets which foster on its characteristics is the propulsion of micro air launch vehicles. In this paper, a set of design options of a hybrid rocket motor is evaluated for propulsion of micro air launch vehicles. In order to evaluate the various design options of a hybrid rocket, we developed design and performance simulation codes. A simulation code is based on a legacy interior ballistic model. MATLAB® environment was used to develop the design and performance analysis codes and to visualize the temporal variation of performance characteristics and grain geometry during burning. We employ the developed codes to assess the replacement of solid rocket motors which are typically used in Air Launch Vehicles by hybrid rocket motors. A typical Micro Air Launch Vehicle mission to launch a 20-kg payload into a 400-km circular polar orbit is assumed. The results show that a hybrid rocket is a suitable candidate for micro air launch vehicles. The performance is improved in terms of specific impulse and thrust with smaller size in the same mission. Several design parameters of hybrid rocket motors were also evaluated and analyzed, including different fuel port geometry, type of fuels and oxidizers, number of ports, nozzle design and initial mass flux. These design parameters bring a significant effect on hybrid rocket performance and size.

KEYWORDS: Hybrid rocket, Micro air launch vehicle, Internal ballistics, Regression rate.

INTRODUCTION

Hybrid rockets are featured with restarting capability, increased safety, high performance and relatively moderate cost. This unique combination of compelling features poses them as prominent candidates to replace solid rocket motors in air-launched tactical missiles and launch vehicles, besides liquid rocket engines in ground-launched strategic missiles and launch vehicles in the near future. A hybrid rocket is comprised of fuel and oxidizer in different physical states, typically a solid fuel and a liquid or gaseous oxidizer. It represents a compromise between a solid rocket motor and a liquid rocket engine (Mingireanu, 2009). In general, hybrid rockets have specific impulse higher than solid rockets and specific impulse density greater than liquid bi-propellant rockets (Kannalath *et al.*, 2003). Wax based hybrid rocket motors are non-toxic, non-hazardous, shippable as freight cargo, potentially carbon neutral and they can be throttled for thrust control or shut down in case of in-flight anomaly then restart on demand (DeSain *et al.*, 2009). In 2004, the Ansari X Prize has put hybrid technology to a brighter future with the successful launch of SpaceShipOne (David, 2004). SpaceShipOne was succeeded by SpaceShipTwo, which is as nearly twice in size and passed the first powered test flight in April 2013.

Despite the advantages of hybrid rockets, there are several shortcomings which are specifically related to overall performance, reliability and cost effectiveness. The overall performance of a hybrid rocket is affected slightly by combustion instabilities and low solid fuel regression rates which require a relatively large fuel surface area to attain the required thrust level (Connell-Jr *et al.*, 2009).

1.International Islamic University Malaysia – Selangor – Malásia
Author for correspondence: Raed Kafafy | IIUM-Mechanical Engineering Department | Jalan Gombak, 50728 | Selayang/Selangor – Malásia | Email: rkafafy@iium.edu.my
Received: 07/31/2013 | **Accepted:** 12/17/2013

The source of combustion instabilities is due to a complex coupling of thermal transients in the solid fuel, the wall heat transfer blocking due to fuel regression rate, and the transients in the boundary layer that forms on the fuel surface (Karabeyoglu *et al.*, 2005). The oxidizer and fuel are unable to mix quickly in a typical hybrid rocket motor, which results in low propellant burning rates causing a reduction in performance (Jacob, 2007).

Problems related to regression enhancement have become a main focus of many researchers. Moreover, there are issues of fuel web burn out, combustion efficiency, combustion stability, throttling characteristics, and nozzle throat material response (Venuopal *et al.*, 2011). Mainly, the performance of a hybrid rocket depends on the regression rate of the motor, which is defined as the rate at which the solid fuel regresses normal to the surface (Kumar and Kumar, 2012). The regression rate can hardly be accurately measured due to high scattering effects. According to interior ballistic model, during combustion, the heat is transferred to the solid surface by convection and radiation, where the solid phase fuel is decomposed. Zilliac and Karabeyoglu (2006) developed a model to predict the regression rate behavior. However, their model is applicable to vaporizing fuels in a cylindrical grain configuration that do not form significant char or melt layers.

In addition to regression rate, there is a fundamental need to evaluate the pressure and the temporal changes of the combusting gas in the engine chamber because they are related to various phenomena such as ignition and extinction, shape change of a fuel grain due to the combustion, instability due to vortices, acoustics, and injectors, and so on.

Several methods were proposed to improve hybrid rockets regression rate such as adopting swirl flow of oxidizers, doping metal additives in fuel composition, using fuel which has melted layer on the fuel surface and designing optimal grain geometry. The swirl flow can increase the residence time (or contact time) of oxidizer stream with fuel surface along the port. Results showed that the average regression rate increases up to 200% as swirl number increases. However, the enhancement of regression rate is severely localized near the inlet of fuel port. Later, the enhancement of regression technique is by employing vortex tube, which have 150% increase in regression rate where the swirl flow dominates over the entire fuel port (Lee *et al.*, 2005). Employing fuel additives, such as ammonium perchlorate (AP), ammonium nitrate (AN) and other nitro-organic compounds, will lower the heat vaporization effectively. This will allow more solid fuel to combust into the flow of oxidizer. The regression rates were also affected by the addition of activated aluminum powder with 20% by weight to increase the fuel mass flux by 70% over that of pure hydroxyl-terminated polybutadiene (HTPB) (Chiaverini *et al.*, 2000). Studies by Karabeyoglu *et al.* (2004) showed that the regression rate of paraffin-based fuels can be increased up to 400% compared to classic fuels such as HTPB (Nakagawa and Hikone, 2011). It is observed that melted-fuel droplets entraining to the gas phase and melted fuel are flowing along the solid-fuel surface. When the oxidizer flows at high speed over the upper side of the melting fuel surface, the surface of the liquid layer becomes unstable, minute wave is formed and tiny droplets are produced at the tips of the wave and supplied to flame zone. This process occurs almost without vaporization (Ishiguro *et al.*, 2011). It is proven experimentally that the melted-fuel flow layer is created on the solid-phase fuel surface and entraining droplets actually exist. The amount of this melted fuel contributes to the high regression rate because it needs less heat flux from the combustion gas flow to promote regression (Nakagawa and Hikone, 2011). The regression rates of the paraffin-based fuels increase as the melted-fuel viscosity decreases (Nakagawa and Hikone, 2011).

Numerous analytical works have been conducted to describe the gaseous flow during the combustion process. Culick (1996) described the mean gaseous flow through the combustion chamber. Saad and Majdalani (2009) developed an analytical model for basic flowfield in hybrid rockets by employing an arbitrary headwall injection which can be used for benchmarking to test large-scale numerical simulations. However, there are limitations because of burning rate sensitivity, complex fluid dynamics and interactions with heat transfer from the flame zone and the fuel surface, viscosity effects on pressure and the mixing of the two streams (Chiaverini and Kuo, 2007).

At Stanford, a group of postgraduate students had launched their 3-inch diameter nitrous oxide/aluminized paraffin hybrid rocket. They have optimized their design by using Gauss-Newton Nonlinear Least Squares (NLSQ) algorithm and used a 4th-order Runge-Kutta method to integrate the equation of motion (McCormick *et al.*, 2004). A genetic algorithm called HYROCS code, developed by researchers at Purdue University, used a different approach to design and optimize hybrid rockets (Schoonover *et al.*, 2000). Therefore, designing a hybrid rocket engine is not a

straight forward process. It is remains challenging because of complexity which involve numerous continuous parameters and variables. There are few published propulsion system design codes available for the industry but many of them employ exhaustive searches in order to optimize continuous variables (Schoonover *et al.*, 2000). During engine operations, both the exposed surface area and perimeter of fuel ports change with time, the mixture ratio will tend to shift even if the oxidizer mass flow is held fixed. High mass flux is desirable in performance to achieve higher volumetric efficiency within the combustion chamber. However, this desire is restricted by the fact that efficient combustion may not be possible at these high mass fluxes and that mixture-ratio shifts become more severe under these conditions (Vonderwell *et al.*, 1995).

We used another approach to examine the performance of a wheel-typed hybrid rocket motor through simulation of different design parameters. This can be integrated with the micro launch air vehicle used in Pegasus. We used the same mission requirement such as same payload, initial mass, required velocity change (ΔV) and altitude to test the hybrid rocket code. We also have evaluated the performance of wheel-typed grain design with the recent used of multiple circular ports. The result showed an improvement on the regression rate. The following section provides a brief description of the design code, followed by a description of the generic simulation algorithm to estimate the performance of the designed hybrid rocket. The next section describes the analysis of the designed hybrid rocket performance through simulation of varying designed parameters. Evaluation section discloses the effects on the regression rate with different geometries.

PRELIMINARY DESIGN OF HYBRID ROCKET

The preliminary design of a hybrid rocket is based on a legacy internal ballistic model (Humble *et al.*, 1995). The algorithm can handle fuel grains with multiple ports of both circular and wheel types. At first, the basic design requirement and reasonable design margins are selected. The design module starts with thermochemical analysis of the hybrid rocket propellant to estimate the main properties of the propellant including specific heat ratio, the molecular mass of combustion products, flame temperature and characteristic velocity. The thermochemical data for LOx/HTPB is obtained from software developed by the National Aeronautics and Space Administration (NASA) which is known as the Chemical Equilibrium with Application (CEA). Frozen-flow approximation is adopted in the model. This should give an optimum oxidizer to fuel ratio (O/F). We further assume that the regression rate is constant at every location during burning while the oxidizer mass flow rate will remain fixed throughout the combustion process. The flowchart of design procedure is shown in Fig. 1.

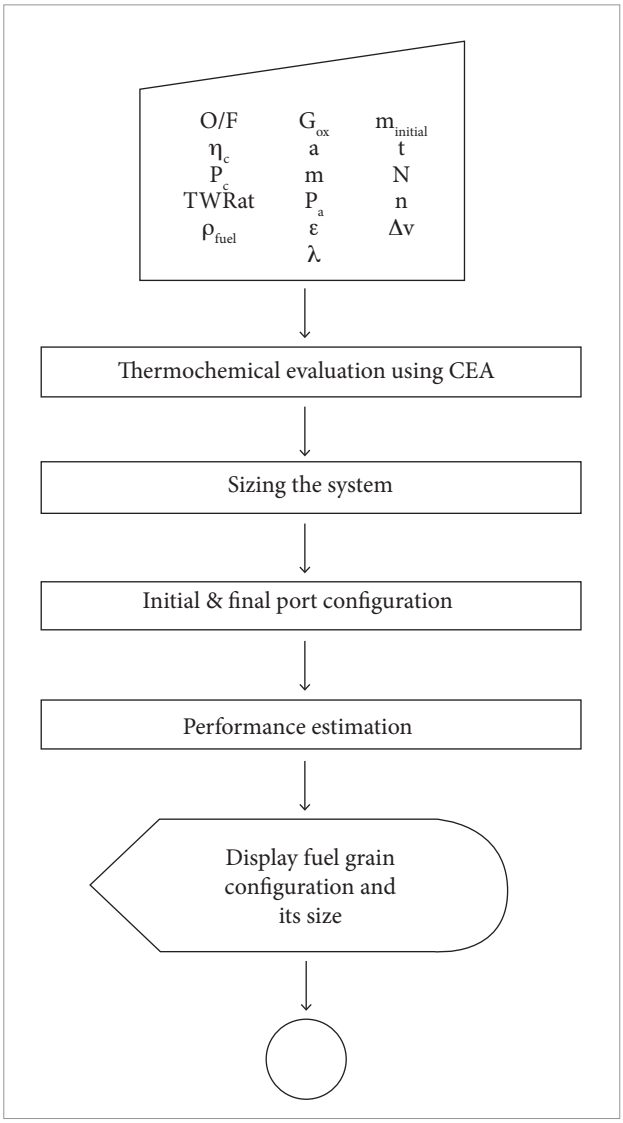

Figure 1. Hybrid rocket preliminary design flowchart.

CEA software requires input of the major and minor species of the chemical reaction, changes of enthalpy and entropy formation of both fuel and oxidizer. The output is the variation of specific heat ratio, molecular weight of the species and the flame temperature with the propellant O/F. Polynomial functions are fitted to the data calculated by CEA for later use in the design and simulation algorithms.

The values of specific heat ratio, molecular weight and flame temperature obtained from CEA are used to calculate the characteristic velocity assuming 98% combustion efficiency.

$$c^* = \frac{\eta_{c^*}\sqrt{\gamma R T_f}}{\gamma\left(\frac{2}{\gamma+1}\right)^{\frac{\gamma+1}{2\gamma-2}}} \quad (1)$$

where c^* is the characteristic velocity, η_{c^*} is the combustion efficiency, γ is the specific heat ratio, R is the gas constant (J/kg.K) and T_f is the flame temperature (K).

The nozzle exit Mach number (M_e) is calculated from the relation of nozzle expansion ratio (ε):

$$\varepsilon = \frac{1}{M_e}\sqrt{\left\{\frac{2}{\gamma+1}\left(1+\frac{\gamma-1}{2}M_e^2\right)\right\}^{\frac{\gamma+1}{\gamma-1}}} \quad (2)$$

The exit pressure (P_e) is calculated using isentropic of chamber pressure (P_c) relation:

$$P_e = \frac{P_c}{\left(1+\frac{\gamma-1}{2}M_e^2\right)^{\frac{\gamma}{\gamma-1}}} \quad (3)$$

Given g_0 is the standard acceleration of gravity, the rocket specific impulse (I_{sp}) is calculated from:

$$I_{sp} = \lambda\left\{\frac{c^*\gamma}{g_0}\sqrt{\left(\frac{2}{\gamma-1}\right)\left(\frac{2}{\gamma+1}\right)^{\frac{\gamma+1}{\gamma-1}}\left[1-\left(\frac{P_e}{P_c}\right)^{\frac{\gamma-1}{\gamma}}\right]}+\frac{c^*\varepsilon}{g_0 P_c}(P_e-P_a)\right\} \quad (4)$$

where λ is the nozzle efficiency and P_a is the ambient pressure.

The combustion chamber pressure is assumed here as a design parameter of the hybrid rocket. The sizing of the overall propulsion system needs the initial mass and total ΔV. For the mission selected here, the mission analysis of the micro air launch vehicle gives a total initial mass of 1,287.34 kg and ΔV of 2,624 m/s (Aldheeb *et al.*, 2012). These values are used to calculate the final mass, propellant mass, fuel mass and fuel mass flux of the hybrid rocket stage using the following relations:

$$m_{final} = m_{initial} e^{\frac{-\Delta v}{I_{sp} g_0}} \quad (5)$$

where m_{final} is the final mass (kg) and $m_{initial}$ is the initial mass (kg).

$$m_{prop} = m_{initial} - m_{final} \quad (6)$$

where m_{prop} is the propellant mass (kg).

$$m_{fuel} = \frac{m_{prop}}{O/F+1} \quad (7)$$

where m_{fuel} is the fuel mass (kg) and O/F is the oxidizer to fuel ratio.

$$G_f = \frac{G_{ox}}{O/F} \quad (8)$$

where G_f is the fuel mass flux (kg/m^2.s) and G_{ox} is the oxidizer mass flux (kg/m^2.s).The grain design of wheel type port configurations can be calculated from the initial oxidizer mass flux and the number of ports. The geometric design of a wheel type fuel grain can be calculated from the following geometric relations. Figure 2 illustrates the geometric parameters used in the geometric relations.

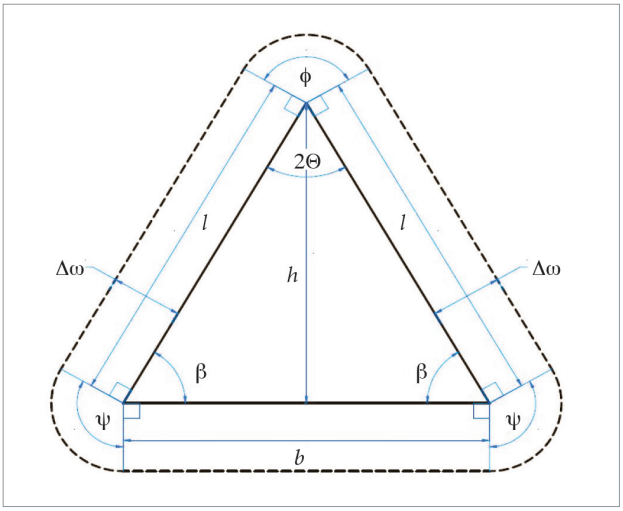

Figure 2. Geometry of a wheel type grain with triangular ports.

$$A_{pi} = \frac{\dot{m}_{oxpp}}{G_{ox}} \quad (9)$$

where A_{pi} is the initial port area (m^2) and $\dot{m}_{oxpp}$ is the oxidizer mass flow rate in each port (kg/s).

$$\theta = \frac{\pi}{N} \quad (10)$$

where θ is the port half angle (degree) and N is the number of ports.

$$h = \sqrt{\frac{A_{pi}}{\tan\theta}} \quad (11)$$

where h is the triangle height (m).

$$b = 2h\tan\theta \quad (12)$$

where b is the length of triangle base (m).

$$l = h/\cos\theta \quad (13)$$

where l is the length of the side triangle (m).

$$P_{pi} = 2l + b \quad (14)$$

where P_{pi} is the initial port perimeter.

$$w^2 + \frac{2l+b}{\pi}w - \frac{m_{fuel}}{N\rho_{fuel}L_p\pi} = 0 \quad (15)$$

where w is the web thickness (m), ρ_{fuel} is the fuel density (kg/m^3) and L_p is the port length (m).

$$r_h = w/\sin\theta - w \quad (16)$$

where r_h is the center hole radius (m).

$$r_g = h + 2w + r_h \quad (17)$$

where r_g is the grain radius (m).

$$A_{throat} = \dot{m}_{prop}\, c^*/P_c \quad (18)$$

where A_{throat} is the throat area (m^2) and $\dot{m}_{prop}$ is the propellant mass flow rate (kg/s).

The length of the fuel grain can be calculated from the following empirical relation:

$$L_p = \left(\frac{\dot{m}_{fuel}}{N\rho_{fuel}a(G_{ox}+G_f)^n P_{pi}}\right)^{\frac{1}{m+1}} \quad (19)$$

where $\dot{m}_{fuel}$ is the fuel mass flow rate (kg/s), m is the fuel length exponent, a is the regression rate coefficient, and n is the mass flux exponent.

The layout of a wheel typed fuel grain with 8 ports, which is obtained by the design code, is shown in Fig. 3.

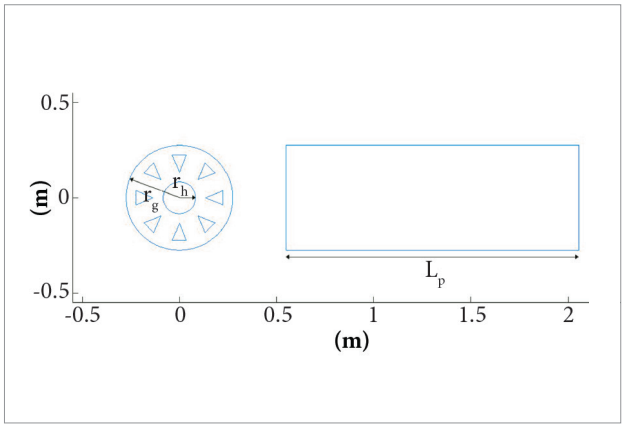

Figure 3. Layout of a wheel type hybrid rocket fuel grain with 8 ports obtained by the design code.

Performance parameters such as the regression rate, exit velocity and thrust are calculated using the following relations. Empirical constants such regression rate coefficient (a), mass flux exponent (n) and length exponent (m) are taken from previous experiment. These values, a = 0.0002, n = 0.75, m = -0.15 and λ=0.9 are obtained from (Humble *et al.*, 1995).

$$Rdot = a(G_{ox} + G_{fuel})^n L_p^m \quad (20)$$

where Rdot is the fuel regression rate (m/s).

$$v_e = \sqrt{\frac{2\gamma RT_o}{(\gamma-1)}\left\{1 - \left(\frac{P_e}{P_o}\right)^{\frac{\gamma-1}{\gamma}}\right\}} \quad (21)$$

where v_e is the exit velocity, T_o is the chamber temperature and P_o is the stagnation pressure (Pa).

$$F = \lambda\left[\dot{m}_{prop}v_e + (P_e - P_a)A_e\right] \quad (22)$$

where F is the thrust force (N) and A_e is the nozzle exit area (m^2).

MICRO AIR LAUNCH VEHICLE USING HYBRID ROCKET MOTOR

We have evaluated hybrid rocket motor performance and size as shown in Table 1. We set the same initial condition and mission requirement as in existing solid rocket motor in MALV for Pegasus XL. For an optimal design of HTPB/LOx, the oxidizer-to-fuel ratio is 2.1, as shown in the thermochemical analysis using CEA. The volume of the oxidizer tank was calculated from mass and density equation and by assuming that the tank is cylindrical. The details of the initial condition and the performance of the designed hybrid rocket motor are given in Table 1.

Table 1. Parameters of the designed hybrid rocket motor for MALV for the first stage.

Parameter	Hybrid Rocket Motor
Optimal O/F	2.1
Specific heat ratio	1.231
Flame temperature (K)	3593.0
Characteristic velocity (m/s)	1747.3
Chamber pressure (MPa)	7.515
Oxidizer mass flux (kg/s/m^2)	300
Thrust (kN)	39.27
Motor length (m)	3.01
Throat area (m^2)	0.0029
Exit area (m^2)	0.1708
Nozzle expansion ratio	58.40
Burning time (s)	45
Fuel diameter (m)	0.66
Initial mass (kg)	1287.34
Propellant mass (kg)	806.97
Specific impulse (s)	316.42
Average regression rate (m/s)	0.00194

SIMULATION OF HYBRID ROCKET PERFORMANCE

The generic simulation algorithm shows the analytical performance of the designed hybrid rocket. Over the period of time, the surface fuel port area will increase due to burning. We assumed that the burning surface will burn perpendicularly and the corner of each port started to have a fillet shape. According to the interior ballistic model, O/F and the geometry of the ports will vary with time. The flowchart of the code is illustrated in Fig. 4.

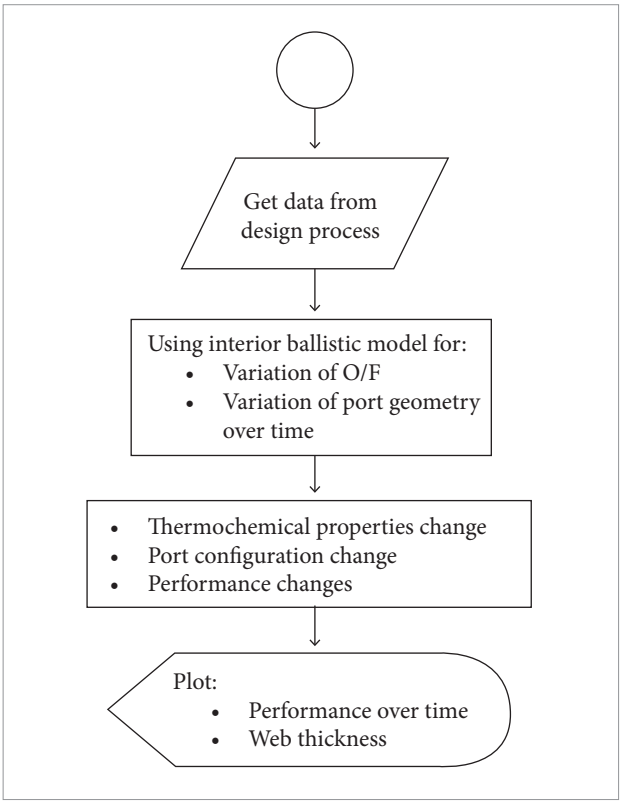

Figure 4. Flowchart of hybrid rocket simulation algorithm.

The simulation algorithm starts by getting values from the output of the design algorithm. During burning, the web thickness decreases continuously and the change in the web section can be estimated from:

$$\Delta w = w_i - \dot{r}\Delta t \tag{23}$$

where Δw is the change of web thickness (m), w_i is the initial web thickness (m) and Δt is the period of time (s).

Angles are formed by assuming that the two side lines and the base is burnt perpendicular leaving each corner a small fillet. The following equations give the angle at each corner of the triangle.

$$\phi = 180 - 2\Theta, \tag{24}$$

where ϕ is the top fillet angle formation (degree).

$$\psi = 90 + \Theta, \tag{25}$$

where ψ is the side fillet angle formation (degree).

As time progresses, the web decreases, forming a new burning surface with varying perimeter and cross sectional area in each port that can be calculated from:

$$Peri_{new} = \left(\frac{\phi}{360} \cdot 2\pi\Delta w\right) + \left(\frac{\psi}{360} \cdot 2\pi\Delta w \cdot 2\right) + (2l) + b \tag{26}$$

where $Peri_{new}$ is the new perimeter formed (m).

$$Ap_{new} = N\left\{\left(\frac{\phi}{360} \cdot \pi\Delta w^2\right) + \left(\frac{\psi}{360} \cdot \pi\Delta w^2 \cdot 2\right) + (b\Delta w) + (2l\Delta w) + A_{pi}\right\} \tag{27}$$

where Ap_{new} is the new total port formed (m^2).

When the port geometry changes, the O/F will vary and, accordingly, the thermochemical properties will change. By using an internal ballistic model for a non-circular type of fuel, the new O/F can be obtained from Eq (28).

$$O/F_{new} = \frac{\dot{m}_{ox}^{1-n} Ap_{new}^{\ n}}{\rho a L_p Peri_{new} N} \tag{28}$$

where O/F_{new} is the new oxidizer to fuel ratio, $\dot{m}_{ox}$ is the oxidizer mass flow rate and ρ is the density of the fuel.

The variation of O/F will affect the performance of the hybrid rocket as well. For simplicity, we assume the oxidizer mass flow rate remains constant throughout burning whereas the fuel mass flow rate is allowed to vary according to this relation:

$$\dot{m}_{fuel} = Rdot \,.\, \rho Peri_{new} L_p N \tag{29}$$

The hybrid rocket O/F, instantaneous web, exit velocity, thrust-to-weight ratio, regression rate and specific impulse are plotted with respect to the time as shown in Fig. 5.

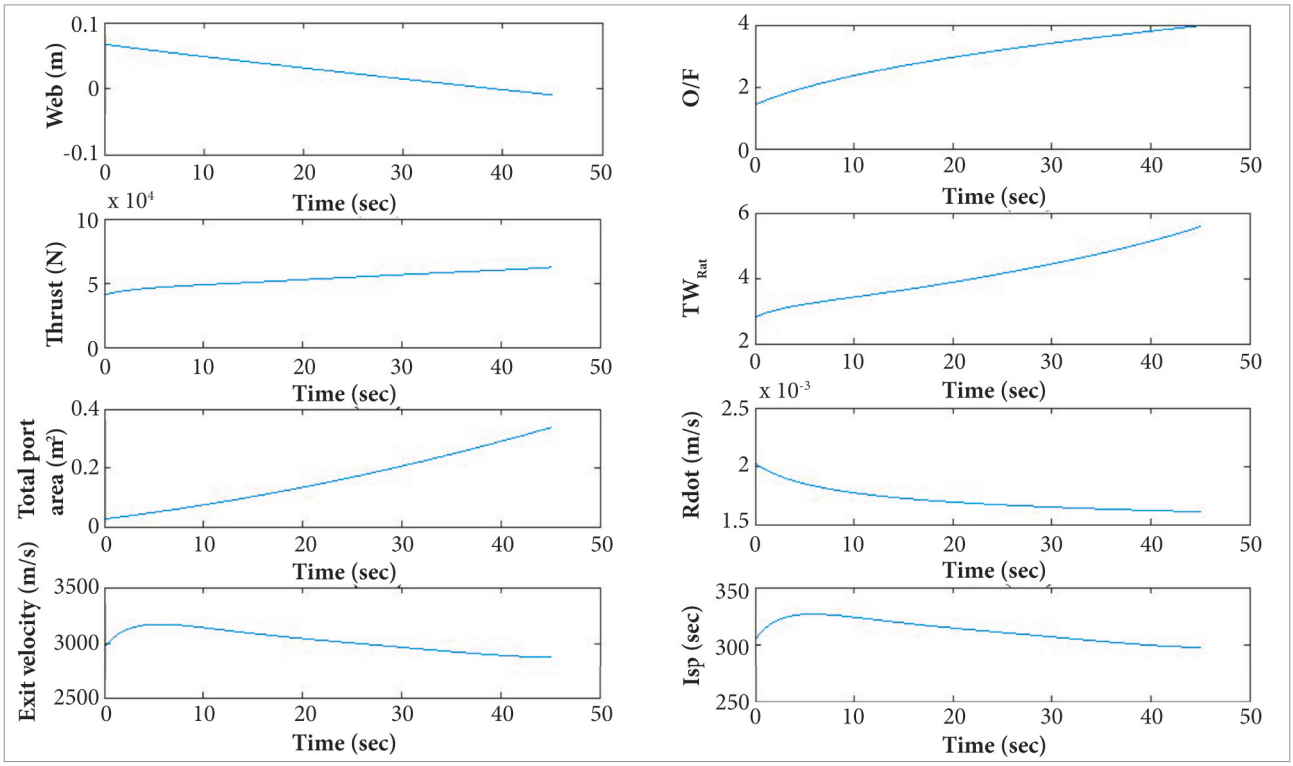

Figure 5. Transient performance of a wheel type hybrid rocket.

A decrease in web thickness is plotted in the top left hand side of the figure. The decreasing in web thickness results in the increase of port area. The changes in the geometry will result in the variation of oxidizer-to-fuel ratio. Notice that the oxidizer-to-fuel ratio increases although the oxidizer mass flow rate is held constant because the port diameter increases with time. The burning rate depends on the regression rate and it is the function of the total mass flux. The regression rate decreases exponentially with time due to changes in mass flux. It is convenient to maintain the regression rate constant along the fuel length at each time step to obtain a small variation of port diameter. The thrust-to-weight ratio increases sharply during the early stage because of the rapid increase in O/F and corresponds to the characteristic velocity. This progressive burning is mainly due to the increase in burning area. However, both specific impulse and exit velocity have a maximum point then started to decrease. The increase in specific impulse at the early stage is dominated by the propellant mass flow rate which is low and, after the increase in the port area, this mass flow rate will start to rise, resulting in a decrease in the total specific impulse. The same goes to the variation of exit velocity which is highly dependent on the chamber pressure and exit conditions.

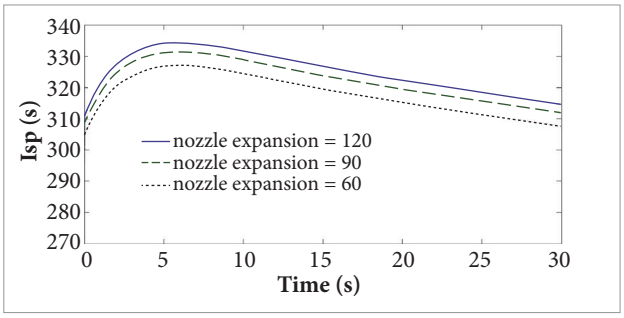

Figure 6. Transient behavior of specific impulse for various nozzle expansion ratios.

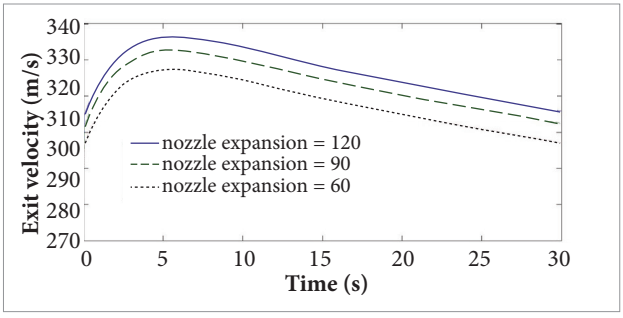

Figure 7. Transient behavior of exit velocity for different expansion ratios.

EFFECT OF VARYING INITIAL DESIGN PARAMETERS ON HYBRID ROCKET PERFORMANCE

We have investigated some of other design features such as nozzle designs with different expansion ratio, different initial oxidizer mass flux, number of ports used and different oxidizers and types of fuels used. These design parameters are based on the user's input. For the purpose of comparison, we maintained the same mission requirement as for micro air launch vehicle. From the results, it proved that these designs will vary its basic performance. Figures 6 and 7 show that, the higher the nozzle expansion ratio, the higher the specific impulse as well as exit velocity. An increase in the nozzle expansion ratio would reduce the exit pressure towards ambient pressure, increasing the thrust coefficient, providing a higher level of thrust, and forcing the system to converge with the predicted results (Terrence *et al*., 2009).

The variation of initial oxidizer mass flux, G_{oi}, will affect the fuel dimension the most. Based on Fig. 8, specific impulse will have less sustainability at higher initial mass flux. The fuel mass flux will have a rapid increase at the early stage and will decrease at some period of time. According to Eq. 20, the regression rate is the function of total mass flux. The total mass flux is the summation of both fuel and oxidizer mass flux. Figure 9 also shows that at higher initial mass flux gives a better thrust-to-weight ratio.

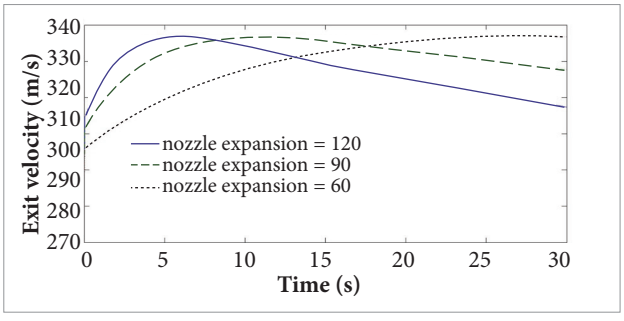

Figure 8. Transient behavior of specific impulse variation for different initial mass fluxes.

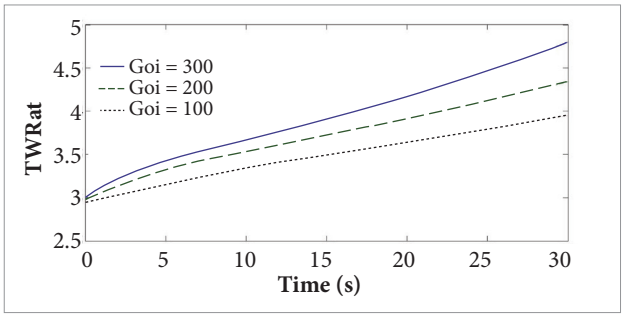

Figure 9. Transient behavior of thrust-to-weight ratio for different initial mass fluxes.

The effect of number of ports on a wheel fuel grain design is discussed and analyzed. The results are shown in Table 2. Multiple ports in fuel grain are desirable to produce larger fuel surface area. The overall performance of hybrid rocket motor is critically depends on the flow mixing degree in the combustion chamber. These multiple combustion ports promote better combustion efficiency due to turbulent mixing environment in the mixing chamber downstream (Sutton and Biblarz, 2001). For many ports design, it showed that the regression rate is improved. However, this requires an increase in the design of grain diameter. Significant increase in chamber diameter indicates a strong increase in regression rate due to the possibility of boundary layer growth with less temperature gradient and more intense radiation heat transfer (Chiaverini and Kuo, 2007).

Figure 10 showed specific impulse variation of different port number. At early burning stage, specific impulse tends to increase rapidly at higher number of ports but it will not sustain longer. The same trend is also shown in Fig. 11 for the exit velocity. Fewer number of ports have its own capability to prolong its impulse but had a slightly decrease. Less number of ports will have larger web thickness, thus have more fuel to keep the fuel burning. The pressure slightly decreased throughout the major portion of the hybrid engine test firing due to volumetric expansion within the combustion chamber and nozzle erosion. The change in cross-section grain area also reduced oxidizer mass flux, which in turn reduces burning rate. Thus, gas production is reduced (Terrence *et al.*, 2009).

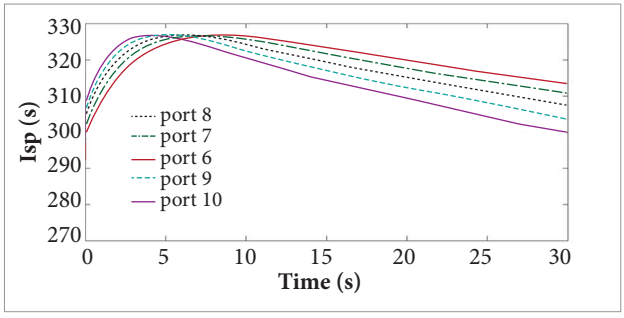

Figure 10. Transient behavior of specific impulse for different number of ports.

Table 2. Variation of performance parameters with number of ports.

Performance parameter	6 ports	7 ports	8 ports	9 ports	10 parts
Fuel length (m)	1.826	1.656	1.506	1.376	1.264
Web (m)	0.069	0.068	0.067	0.067	0.067
Fuel volume per port (m^3)	0.064	0.055	0.048	0.043	0.039
Final area of port (m^2)	0.042	0.037	0.035	0.034	0.033
Final perimeter of port (m)	0.705	0.682	0.666	0.654	0.645
Final surface area of port (m^2)	1.288	1.129	1.003	0.881	0.816
Radius of center hole (m)	0.068	0.088	0.109	0.129	0.153
Radius of grain (m)	0.292	0.311	0.332	0.352	0.373
Regression rate (cm/s)	0.208	0.211	0.214	0.217	0.219

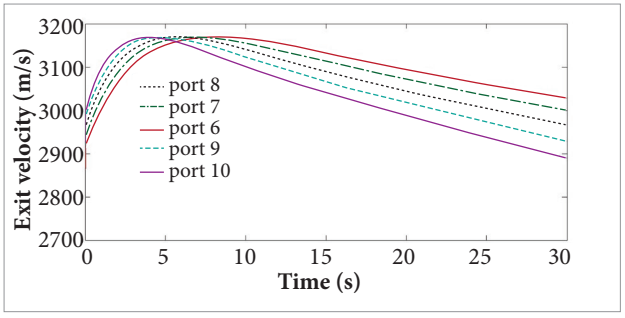

Figure 11. Transient behavior of exit velocity for different number of ports.

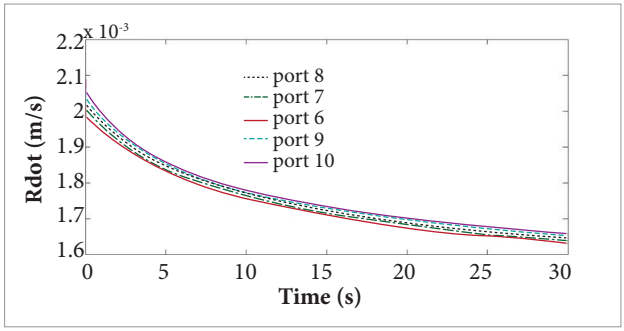

Figure 12. Transient behavior of regression rate for different number of ports.

Many ports have better regression rate and more fuel can be decomposed as shown in Fig. 12, but it requires more weight for the structural design. Fewer ports have lighter weight on its structural design, but the regression rate is lower. These conditions resulted in little variation between different port designs.

The effect of varying the oxidizer on performance is analyzed. Different oxidizers with HTPB fuel were considered, namely oxygen (LOx), hydrogen peroxide (H_2O_2) and nitrogen tetroxide (N_2O_4). The results show that the performance was mainly influenced by the thermo chemical properties of the fuel/oxidizer mixture. Liquid oxygen has lower boiling point and density compared to hydrogen peroxide. The HTPB and liquid oxygen provides a relatively high regression rate with a relatively stable burn (Mingireanu, 2009). Thermochemistry properties and curve fit relation for hydrogen peroxide and nitrogen tetroxide adopted from Humble *et al.* (1995) and CEA. The properties of candidate oxidizers and fuels are given in Tables 3 and 4.

Figure 13 shows that liquid oxygen oxidizer gives the highest specific impulse. Nevertheless, it has an optimum value until it drops at a certain time. However, hydrogen peroxide has better thrust-to-weight ratio compared to other oxidizers as shown in Fig. 14. Liquid oxygen gives a better thrust during the early stage while nitrogen tetroxide gives the lowest value during the burn. Liquid oxygen and hydrogen peroxide give a better improvement on the regression rate. This proved that the choice of oxidizers bring impact on regression enhancement.

Table 3. Properties of oxidizers.

Oxidizer	Chemical formula	T_{FP} (K)	T_{BP} (K)	P_{vap} (MPa)	Density (kg/m³)	Heat of formation (cal/g)
Oxygen	O_2	54	90	5.07 @ 154K	1142	0
Hydrogen peroxide	H_2O_2	267.4	419	0.345 @ 298K	1414	-1440 (90%HP) -1340 (98%HP)
Nitrogen tetroxide	N_2O_4	261	294	0.765 @ 344K	1440	-50.9
Nitrous oxide	N_2O	182.29	184.67	5.15@ 293K	102	443

T_{FP}: freezing point temperature; T_{BP}: boiling point temperature; P_{vap}: vapour pressure.

Table 4. Properties of fuels.

Fuel	Chemical formula	T_{Melt} (K)	T_{BP} (K)	Density (kg/m³)	Enthalpy of formation (kJ/mol)
HTPB	$C_{10}H_{15}.4\,O_0.O7$	514.15	N/A	920	-51.9
Paraffin wax	$C_{28}H_{58}$	327.55	438.89 @ 1atm	809	-1438.2

T_{Melt}: melting temperature; T_{BP}: boiling point temperature.

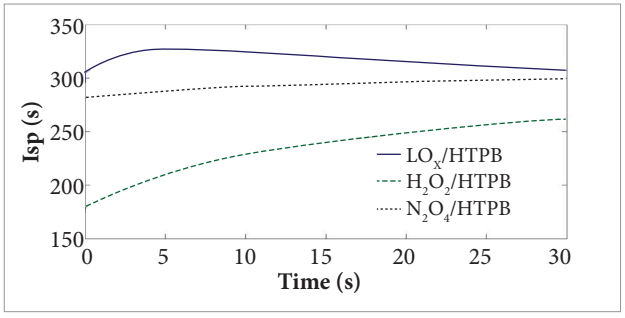

Figure 13. Transient behavior of specific impulse for different types of oxidizer.

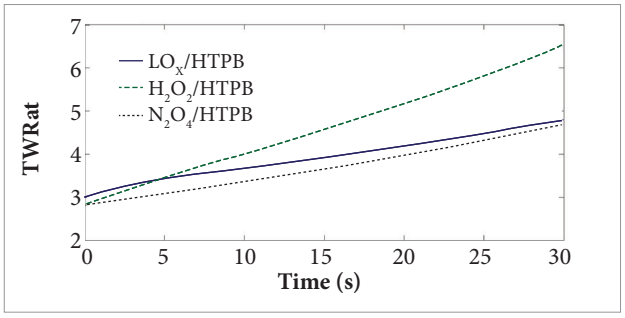

Figure 14. Transient behavior of thrust-to-weight ratio for different types of oxidizer.

We have also compared the performance with different types of fuels such as Paraffin and conventionally used HTPB with nitrous oxide as an oxidizer. Paraffin based fuel shows regression rate enhancement as in Fig. 15. This is numerically proven on experimental works carried out by previous researchers at Stanford University. This fast burning fuels form a hydro dynamically unstable liquid layer over the surface which encourages high regression rate (Karabeyoglu *et al.*, 2004).

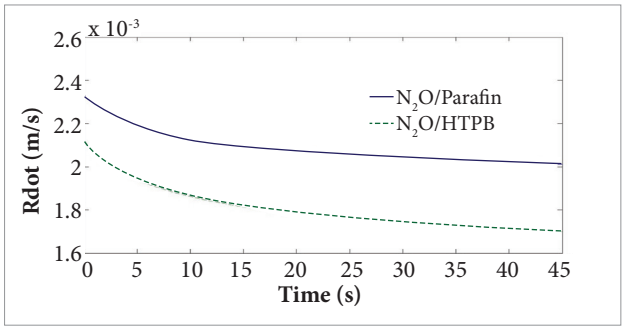

Figure 15. Transient behavior of regression rate for different types of fuels.

Figure 16 shows an inverse effect of using different types of fuels. Paraffin fuel gives a decrease in specific impulse over time. This trend occurs because of thermochemical properties of both types of fuels. Values of a and n parameters, appearing in Eq. 20 for N_2O/Paraffin and N_2O/HTPB are a = 0.488, n = 0.62 (Karabeyoglu *et al.*, 2004) and a = 0.198, n = 0.325 (Lee and Tsai, 2009).

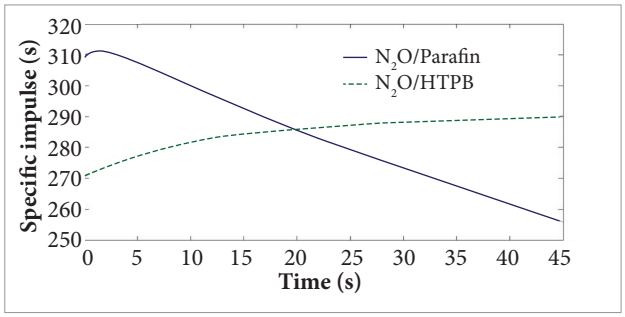

Figure 16. Transient behavior of specific impulse for different types of fuels.

EVALUATION OF WHEEL-TYPED AND MULTIPLE CIRCULAR PORTS PERFORMANCE

Table 5 shows that wheel-typed port requires a larger grain diameter but less fuel length for the desired thrust. Wheel-typed port with thicker web has an advantage for longer burning time. Moreover, wheel-typed ports have better burning port surface with at least 30% increase. This results show 5% increase of the average regression rate. However, studies showed that for short fuel grains, the boundary layer will not fully develop along the port longitudinal axis and some of the downstream parts of the fuel grain will gasify without complete burning while long grains, the entire oxidizer will be consumed before reaching the end of the grain (Kannalath *et al.*, 2003).

To estimate the final grain diameter at each port we use:

$$D_{pf} = \sqrt{\frac{4m_{fuel}}{\pi L_p \rho N} + D_{pi}^2} \qquad (30)$$

where D_{pf} is the final diameter of port (m) and D_{pi} is the initial diameter of port (m).

Table 5. Comparison of multiple-circular ports and wheel-typed ports design for 8 ports.

	Multiple-circular	Wheel-typed
Grain diameter (m)	0.6	0.66
Fuel length (m)	2.073	1.506
Web thickness (m)	0.06	0.0673
Final area of each ports (m^2)	0.027	0.035
Final surface area of each ports (m^2)	1.197	1.003
Average regression rate (m/s)	0.00204	0.00214

$$w = \frac{D_{pf} - D_{pi}}{2} \tag{31}$$

The analytical solution for circular ports with constant oxidizer mass flow is:

$$\int_{D_{pi}}^{D_p} D_p^{2n} dD_p = 2a\left(\frac{4\dot{m}_{ox}}{\pi}\right)^n L_p^m \int_0^t dt \tag{32}$$

where D_p is the diameter of port.

For plotting at any time, the variation of grain diameter uses this relation:

$$D_p = \left(a(4n+2)\left(\frac{4\dot{m}_{ox}}{\pi}\right)^n L_p^m t + D_{pi}^{2n+1}\right)^{\frac{1}{2n+1}} \tag{33}$$

Using the ballistic model, the variation of O/F for circular ports is:

$$O/F_{new} = \frac{\dot{m}_{ox}^{1-n} D_p^{2n-1}}{4^n \rho \pi^{1-n} a L_p N} \tag{34}$$

Figures 17, 18 and 19 show a comparison of both grain designs in terms of its specific impulse, the regression rate and thrust-to-weight ratio. In Fig. 17, multiple circular ports show better improvement of specific impulse. This is probably caused by the fast change in the geometrical area.

Figure 18 shows a clear improvement on the regression rate of the wheel-typed grain. As the time goes, the surface burning area becomes much larger compared to the circular ports, but both designs show a decline trend due to a decrease of mass flux. Both designs show a regressive burning where the thrust decreases over the time. However, wheel-typed grain has an increase on thrust-to-weight ratio compared to the circular ports. More fuel is burnt in the wheel-typed grain due to a larger burning surface area.

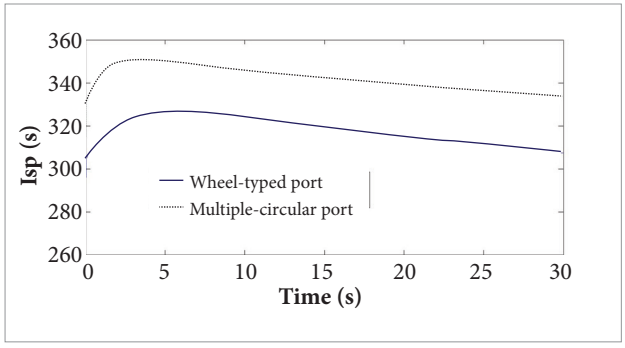

Figure 17. Transient behavior of specific impulse for different fuel grain types.

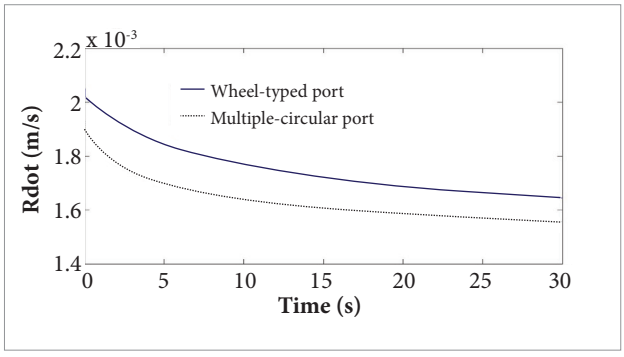

Figure 18. Transient behavior of regression rate for different fuel grain types.

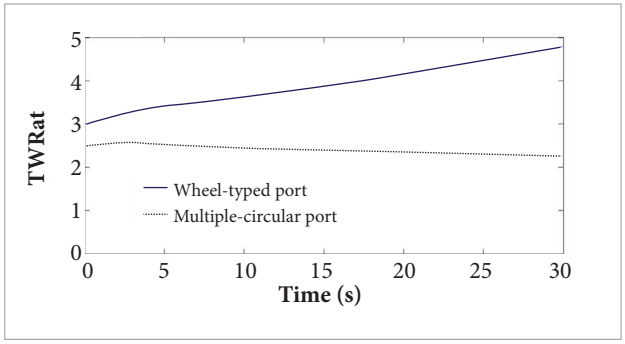

Figure 19. Transient behavior of thrust-to-weight ratio for different fuel grain design.

CONCLUSION

The designed code and generic algorithm analytical performance simulation of hybrid rockets was developed and successfully demonstrated. Prior to the code, we have shown the effect of varying design parameters which can continuously change the performance. Hybrid rocket designers have to properly select and decide to meet the mission requirements. Since this code is developed for the design of propulsion system, it will require further modifications to include all factors needed by space mission analysts and designers.

Based on the obtained results, the choice of initial mass flux determines its performance sustainability. According to the temporal variation, higher initial mass flux will give a rapid increase on its performance, but will not sustain longer. The choice of number of ports also plays an important role in determining the hybrid rocket performance. Many ports have better regression rate and thrust but encounter structural integrity problem.

In general, the wheel-typed grain design has higher regression rate and higher thrust-to-weight ratio compared to the multiple circular ports, but it requires a larger grain diameter. As the results showed, grain geometry has a profound effect on regression rate. Larger surface area is preferable but it has structural limitations. A conventionally used multiple-circular port has better structural integrity but lack of performance. Hybrid rocket designers have to compromise these effects to achieve the mission requirement for a micro air-launch vehicle.

REFERENCES

Aldheeb, M.A., Kafafy, R.I., Idres, M., Omar, H.M. and Abido, A.M., 2012, "Design Optimization of Micro Air Launch Vehicle Using Different Evolution", Journal of Aerospace Technology and Management, Vol. 4, No. 2, pp. 185-196. doi: 10.5028/jatm.2012.04020112.

Chiaverini, M.J. and Kuo, K.K., 2007, "Fundamentals of Hybrid Rocket Combustion and Propulsion", American Institute of Aeronautics and Astronautics, Virgina, USA.

Chiaverini, M. J., Serin, N., Johnson, D. K., Lu, Y.-C., Kuo, K. K. and Risha, G.A., 2000, "Regression Rate Behaviour of Hybrid Rocket Solid Fuels", Journal of Propulsion and Power, Vol. 16, No. 1, pp. 125-132.

Connell-Jr, T.L., Santi, S.A., Risha, G.A., Muller, B.A. and Batzel, T.D., 2009, "Experiment and Semi-Experiment Modeling of Lab-Scale Hybrid Rocket Performance", 45th AIAA/ASME/SAE/ASEE Joint Propulsion Conference & Exhibit. Denver, Colorado.

Culick, F. E. C., 1966, " Rotational axisymmetric mean flow and damping of acoustic waves in a solid propellant rocket", AIAA Journal, Vol. 4, No 8, pp. 1462-1464.

David, L., 2004, "SpaceShipOne Wins $10 Million Ansari X Prize in Historic 2nd Trip to Space", Retrieved in January 10, 2012, from http://www.space.com/403-spaceshipone-wins-10-million-ansari-prize-historic-2nd-trip-space.html.

DeSain, J.D., Brady, B.B., Metzler, K.M., Curtiss, T.J. and Albright, T.V., 2009, "Tensile Tests of Paraffin Wax for Hybrid Rocket Fuel Grains", 45th AIAA/ASME/SAE/ASEE Join Propulsion Conference & Exhibit, Denver, Colorado.

Humble, R.W., Henry, G.N. and Larson, W.J., 1995, "Space Propulsion Analysis and Design", Ed. McGraw-Hill, USA.

Ishiguro,T., Keizi Sinohara, K.S. and Nakagawa, I., 2011, "A Study on Combustion Efficiency of Paraffin-based Hybrid Rockets", 47th AIAA/ASME/SAE/ASEE Joint Propulsion Conference & Exhibit, San Diego, California.

Jacob, E., 2007, "The Effect of Oxidizer Laced Hybrid Rocket Regression Rates and Performance", American Institute of Aeronautics and Astronautics (AIAA) Southeastern Regional Student Conference, Savannah, Georgia.

Kannalath, R., Kuznetsov, A. and Natan, B., 2003, "Design of a Lab-scale Hydrogen Peroxide/Hydroxyl Terminated Polybutadiene Hybrid Rocket Motor", 39th AIAA/ASME/SAE/ASEE Joint Propulsion Conference & Exhibit. Alabama.

Karabeyoglu, A., Zilliac, G., Cantwell, B. J., DeZilwa, S. and Castellucci, P., 2004, "Scale-Up Tests of High Regression Rate Paraffin-Based Hybrid Rocket Fuels", Journal of Propulsion and Power, Vol. 20, No. 6, pp. 1037-1045. doi: 10.2514/1.3340.

Karabeyoglu, M., Zilwa, S., Cantwell, B. and Zilliac, G., 2005, "Modelling of Hybrid Rocket Low Frequency Instabilities", Journal of Propulsion and Power, Vol. 21, No. 6, pp. 1107-1116. doi: 10.2514/1.7792.

Kumar, C. P. and Kumar, A., 2012, "A Numerical Study on the Regression Rate of Hybrid Rocket Motors Using a Combination of Enhancement Techniques", 48th AIAA/ASME/SAE/ASEE Joint Propulsion Conference & Exhibit, Atlanta, Georgia.

Lee, C., Na, Y. and Lee, G., 2005, "The Enhancement of Regression Rate of Hybrid Rocket Fuel by Helical Grain Configuration and Swirl Flow", 41st AIAA/ASME/SAE/ASEE Joint Propulsion Conference & Exhibit, Tucson, Arizona.

Lee, J., Moon, H., Sung, H., Kim, J. and Park, S., 2011, "Combustion Characteristics of Initial Port Diameter Variation of Solid Fuel in Hybrid Rocket Motor", 47th AIAA/ASME/SAE/ASEE Joint Propulsion Conference & Exhibit. San Diego, California.

Lee, T.-S. and Tsai, H.-L., 2009, "Fuel Regression Rate in a Paraffin-HTPB Nitrous Oxide Hybrid Rocket", 7th Asia-Pacific Conference on Combustion, Taipei.

McCormick, A., Hultgren, E., Lichtman, M., Smith, J., Sneed, R. and Azimi, S., 2004, "Design, Optimization, and Launch of a 3" Diameter N20/Aluminized Paraffin Rocket", AIAA.

Mingireanu, F., 2009, "Hybrid rocket motor internal ballistic model and oxidizer dopping. Applications", 4th International Conference on Recent Advances in Space Technologies – RAST '09, Istanbul.

Nakagawa, I. and Hikone, S., 2011, "Study on the Regression Rate of Paraffin-Based Hybrid Rocket Fuels", Journal of Propulsion and Power, Vol. 27, No. 6, pp. 1276-1279. doi: 10.2514/1.B34206.

Saad, T. and Majdalani, J., 2009, "Rotational flowfields in porous channels with arbitrary headwall injection", Journal of Propulsion and Power, Vol.25, No 4, pp. 921-929.

Schoonover, P.L., Crossley, W.A. and Heister, S.D., 2000, "Application of a Genetic Algorithm to the Optimization of Hybrid Rockets", Journal of Spacecraft and Rockets, Vol. 37, No. 5, pp. 622-629. doi: 10.2514/2.3610.

Sutton, G.P. and Biblarz, O., 2001, "Rocket Propulsion Element", Ed. John Wiley & Sons, Canada.

Terrence, L., Connell, J., Santi, S.A., Risha, G.A., Muller, B.A. and Batzel, T.D., 2009, "Experiment and Semi-Experiment Modeling of Lab-Scale Hybrid Rocket Performance", 45th AIAA/ASME/SAE/ASEE Joint Propulsion Conference & Exhibit, Denver, Colorado.

Venuopal, S., Rajesh, K. and Ramanujachari, V., 2011, "Hybrid Rocket Technology", Defense Science Journal, Vol. 61, No. 3, pp. 193-200.

Vonderwell, D.J., Murray, I.R. and Heister, S.D., 1995, "Optimization of Hybrid-Rocket-Booster Fuel-Grain Design", Journal of Spacecraft and Rockets, Vol. 32, No. 6, pp. 964-969. doi: 10.2514/3.26716.

Zilliac, G. and Karabeyouglu, M., 2006, "Hybrid Rocket Fuel Regression Rate Data and Modelling", 42nd AIAA/ASME/SAE/ASEE Joint Propulsion Conference & Exhibit, California.